# Phase diagram of neutral quark matter in nonlocal chiral quark models

D. Gómez Dumm $^{a,b}$ , D.B. Blaschke $^{c,d}$ , A.G. Grunfeld $^e$  and N.N. Scoccola $^{b,e,f}$ 

```
    a IFLP, CONICET - Dpto. de Física, Universidad Nacional de La Plata, C.C. 67, 1900 La Plata, Argentina
    b CONICET, Rivadavia 1917, 1033 Buenos Aires, Argentina
    c Gesellschaft für Schwerionenforschung (GSI) mbH, Planckstr. 1, D-64291 Darmstadt, Germany
    d Bogoliubov Laboratory for Theoretical Physics, JINR Dubna, 141980 Dubna, Russia
    e Physics Department, Comisión Nacional de Energía Atómica,
    Av. Libertador 8250, 1429 Buenos Aires, Argentina
    f Universidad Favaloro, Solís 453, 1078 Buenos Aires, Argentina
```

We consider the phase diagram of two-flavor quark matter under neutron star constraints for two nonlocal, covariant quark models within the mean field approximation. In the first one (Model I) the nonlocality arises from the regularization procedure, motivated by the instanton liquid model, whereas in the second model (Model II) a separable approximation of the one-gluon exchange interaction is applied. We find that Model II predicts a larger quark mass gap and a chiral symmetry breaking (CSB) phase transition line which extends 15-20 % further into the phase diagram spanned by temperature (T) and chemical potential ( $\mu$ ). The corresponding critical temperature at  $\mu=0$ ,  $T_c(0)\simeq 140$  MeV, is in better accordance to recent lattice QCD results than the prediction of the standard local NJL model, which exceeds 200 MeV. For both models we have considered the case of low, standard and large coupling strengths in the scalar diquark channel, showing that different low-temperature quark matter phases can occur at intermediate densities: normal quark matter (NQM) phase, superconducting (2SC)-NQM mixed phase and pure 2SC phase, respectively. Although in most cases there is also a gapless 2SC phase, this occurs mainly in small regions at nonzero temperatures, thus no significant effect should be expected for compact star applications.

PACS numbers: 12.38.Mh, 24.85.+p, 26.60.+c, 97.60.-s

### I. INTRODUCTION

Within the last decade the investigation of the thermodynamics and phase structure of strongly interacting matter has been driven by the results of the experimental programs with ultrarelativistic heavy ion beams at CERN-SPS and BNL-RHIC [1] as well as by the unprecedented quality of data from lattice QCD simulations [2]. A new picture of the state of matter created in these experiments has emerged, according to which the physical nature of the sought-for quark-gluon plasma (QGP) is a perfect liquid of strongly correlated hadron-like resonances rather than an ideal gas of quasifree quarks and gluons [3, 4]. The persistence of a strong, nonperturbative coupling in the QGP can be supposed as a prerequisite of a successful modelling of the QCD phase diagram. Turning to the domain of finite chemical potentials, guidance from lattice QCD is limited to  $\mu \leq T$  (where Taylor expansion techniques can be applied), and experimental programmes such as CBM at FAIR Darmstadt are yet in the stage of preparation with a planned begin of operation in 2014. Therefore, predictions for the QCD thermodynamics at low temperatures and high baryon densities  $\mu \geq T$ , where the critical point and the regions of color superconducting quark matter are expected in the QCD phase diagram [5], have to be developed within effective models for strongly coupled, nonperturbative QCD and to be tested against observational constraints from neutron stars [6].

For two-flavor isospin symmetric quark matter the QCD phase diagram has been explored in the frame of different quark models. All of them agree in finding that the two-flavor color superconducting phase (2SC) occurs at low temperatures and moderate chemical potentials [7]. However, when different chemical potentials are considered for each quark flavor and color, and compact star conditions are imposed —i.e., color and electric charge neutrality conditions, together with  $\beta$  equilibrium—, the situation is more complicated and different models lead to qualitatively different results. For example, in Ref. [8] the authors claim that the 2SC phase would be disfavored against the color-flavor-locking (CFL) one in the interior of neutron stars if these conditions are imposed. In contrast, results from models with selfconsistently determined quark masses [9, 10] indicate that the appearance of the 2SC phase is favored in an intermediate regime of densities before free strange quarks appear in the system. In this case, however, for intermediate coupling the authors only find a somewhat narrow region of a gapless 2SC (g2SC) phase [11] at intermediate temperatures and chemical potentials. There are also some results arising from a noncovariant nonlocal quark model [12, 13] which show that the 2SC phase is not present in asymmetric quark matter for standard values of the diquark coupling, considering Gaussian regulator functions [14]. In this model, for strong diquark couplings one does find a 2SC phase, together with a g2SC and a mixed normal quark matter (NQM)-2SC phase in which the electric charge neutrality is satisfied only at a global level [15, 16, 17].

Given this variety of qualitatively different results, it is important to investigate the situation in the case of effective models that go beyond those used in Refs. [8, 10, 14], in the sense that they include fully covariant nonlocal interactions. Nonlocality arises naturally in the context of several quite successful approaches to low energy quark dynamics as, for example, the instanton liquid model [18] and the Schwinger-Dyson resummation techniques [19]. The same happens in lattice QCD [20]. It has been also argued that nonlocal models have several advantages over the local ones (e.g., the Nambu-Jona-Lasinio model [21] and its generalizations). Indeed, nonlocal interactions regularize the model in such a way that anomalies are preserved [22] and charges properly quantized, the effective interaction is finite to all orders in the loop expansion and there is not need to introduce extra cut-offs, soft regulators such as Gaussian functions lead to small next-to-leading order corrections [23, 24], etc. This type of models has been successfully used to investigate meson [25, 26, 27, 28] and baryon [29, 30, 31] properties at vanishing temperature and chemical potential. The phase diagram of isospin symmetric matter has also been studied within this context [32, 33, 34, 35, 36]. The aim of the present work is to extend these analyses to the case in which compact star conditions are imposed.

The paper is organized as follows. In Section II we introduce the model and derive some useful analytical expressions. In Section III we present the numerical results obtained for the case of a Gaussian regulator, considering different ratios between the coupling constants. Then, in Section IV we discuss the features of the obtained phase diagrams, and in Section V we present our conclusions.

### II. FORMALISM

Let us begin by stating the Euclidean action for the nonlocal chiral quark model in the case of two light flavors and anti-triplet diquark interactions,

$$S_E = \int d^4x \, \left\{ \bar{\psi}(x) \left( -i\partial \!\!\!/ + m \right) \psi(x) - \frac{G}{2} j_M^f(x) j_M^f(x) - \frac{H}{2} \left[ j_D^a(x) \right]^{\dagger} j_D^a(x) \right\} \,. \tag{1}$$

Here m is the current quark mass, which is assumed to be equal for u and d quarks. The nonlocality can be introduced now in different ways [37]. In what follows we will work within two alternative scenarios, that we call "Model I" and "Model II", in which the currents  $j_{M,D}(x)$  in Eq.(1) are given by nonlocal operators. In the case of Model I [26, 27], the effective interactions are based in an instanton liquid picture of QCD. The nonlocal currents read

$$j_{M}^{f}(x) = \int d^{4}y \ d^{4}z \ r(y-x) \ r(x-z) \ \bar{\psi}(y) \ \Gamma_{f} \ \psi(z),$$
  
$$j_{D}^{a}(x) = \int d^{4}y \ d^{4}z \ r(y-x) \ r(x-z) \ \bar{\psi}_{C}(y) \ i\gamma_{5}\tau_{2}\lambda_{a} \ \psi(z),$$
 (2)

where we have defined  $\psi_C(x) = \gamma_2 \gamma_4 \bar{\psi}^T(x)$  and  $\Gamma_f = (1, i\gamma_5 \vec{\tau})$ , while  $\vec{\tau}$  and  $\lambda_a$ , with a = 2, 5, 7, stand for Pauli and Gell-Mann matrices acting on flavor and color spaces, respectively.

On the other hand, Model II [25, 38] arises from a separable form of effective one-gluon exchange picture. The nonlocal currents  $j_{M,D}(x)$  in this case are given by

$$j_M^f(x) = \int d^4z \ g(z) \ \bar{\psi}(x + \frac{z}{2}) \ \Gamma_f \ \psi(x - \frac{z}{2}) ,$$

$$j_D^a(x) = \int d^4z \ g(z) \ \bar{\psi}(x + \frac{z}{2}) \ i\gamma_5 \tau_2 \lambda_a \ \psi(x - \frac{z}{2}) .$$
(3)

The functions r(x-y) and g(z) in Eqs. (2) and (3) are nonlocal regulators characterizing the corresponding interactions. It is convenient to translate them into momentum space. Since Lorentz invariance implies that they can only be functions of  $p^2$ , we will use for the Fourier transforms of these regulators the forms  $r(p^2)$  and  $g(p^2)$  from now on.

The effective action in Eq. (1) might arise via Fierz rearrangement from some underlying more fundamental interactions, and is understood to be used —at the mean field level— in the Hartree approximation. In general, the ratio of coupling constants H/G would be determined by these microscopic couplings; for example, OGE interactions, as well as instanton model interactions, lead to H/G = 0.75. However, since the precise derivation of the effective couplings from QCD is not known, there is a significant theoretical uncertainty in this value. In fact, so far there is no strong phenomenological constraint on H/G, except for the fact that values larger that  $H/G \sim 1$  are quite unlikely to be realized in QCD, since they might lead to color symmetry breaking in the vacuum. We will leave the ratio as a free parameter, analyzing the results obtained for values lying within a range from 0.5 to 1.

The partition function of the system at temperature T and quark chemical potentials  $\mu_{fc}$  is given by

$$\mathcal{Z} = \int \mathcal{D}\bar{\psi}\mathcal{D}\psi \ e^{-S_E(\mu_{fc},T)} \ , \tag{4}$$

where the Euclidean action is obtained from Eq. (1) by going to momentum space and performing the replacements

$$p_4 \rightarrow \omega_n - i\mu_{fc} , \qquad \int \frac{d^4p}{(2\pi)^4} \rightarrow T \sum_{n=-\infty}^{\infty} \int \frac{d^3\vec{p}}{(2\pi)^3} .$$
 (5)

Here  $p_4$  is the fourth component of the (Euclidean) momentum of a quark carrying flavor f and color c, and  $\omega_n$  are the Matsubara frequencies corresponding to fermionic modes,  $\omega_n = (2n+1)\pi T$ . We are assuming here that quark interactions depend on the temperature and chemical potentials only through the arguments of the regulators. Note that, as required for the applications we are interested in, we have introduced in Eq. (4) different chemical potentials for each quark flavor and color.

To proceed it is convenient to perform a standard bosonization of the theory. Thus, we introduce the bosonic fields  $\sigma$ ,  $\pi_a$  and  $\Delta_a$ , and integrate out the quark fields. In what follows we work within the mean field approximation (MFA), in which these bosonic fields are replaced by their vacuum expectation values  $\bar{\pi}_a = 0$ ,  $\bar{\sigma}$  and  $\bar{\Delta}_a$ . Moreover, we adopt the usual 2SC ansatz  $\bar{\Delta}_5 = \bar{\Delta}_7 = 0$ ,  $\bar{\Delta}_2 = \bar{\Delta}$ . Within this approximation, and employing the Nambu-Gorkov formalism, the mean field thermodynamical potential per unit volume can be written as

$$\Omega^{MFA} = -\frac{T}{V} \ln \mathcal{Z}^{MFA} = \frac{\bar{\sigma}^2}{2G} + \frac{|\bar{\Delta}|^2}{2H} - \frac{T}{2} \sum_{n=-\infty}^{\infty} \int \frac{d^3 \vec{p}}{(2\pi)^3} \ln \det \left[ \frac{1}{T} S^{-1}(\bar{\sigma}, \bar{\Delta}) \right] . \tag{6}$$

Here the inverse propagator  $S^{-1}(\bar{\sigma}, \bar{\Delta})$  is a 48 × 48 matrix in Dirac, flavor, color and Nambu-Gorkov spaces, given by

$$\begin{pmatrix}
-\not p_{ur}^+ + \Sigma_{ur} & 0 & 0 & 0 & 0 & 0 & \gamma_5 \tau_2^c \Delta & 0 \\
0 & -\not p_{ub}^+ + \Sigma_{ub} & 0 & 0 & 0 & 0 & 0 & 0 & 0 \\
0 & 0 & -\not p_{dr}^+ + \Sigma_{dr} & 0 & -\gamma_5 \tau_2^c \Delta^* & 0 & 0 & 0 & 0 \\
0 & 0 & 0 & -\not p_{dr}^+ + \Sigma_{db} & 0 & 0 & 0 & 0 & 0 \\
0 & 0 & 0 & \gamma_5 \tau_2^c \Delta^* & 0 & -\not p_{ur}^- + \Sigma_{ur}^* & 0 & 0 & 0 & 0 \\
0 & 0 & 0 & 0 & 0 & -\not p_{ub}^- + \Sigma_{ub}^* & 0 & 0 & 0 \\
-\gamma_5 \tau_2^c \Delta & 0 & 0 & 0 & 0 & -\not p_{dr}^- + \Sigma_{dr}^* & 0 & 0 \\
0 & 0 & 0 & 0 & 0 & 0 & -\not p_{dr}^- + \Sigma_{dr}^* & 0
\end{pmatrix}$$
(7)

where we have used the definitions

$$p_{fc}^{\pm} = \left( \omega_n \mp i \,\mu_{fc} \,,\, \vec{p} \,\right) \,, \tag{8}$$

$$\Sigma_{fc} = m + \bar{\sigma} h(p_{fc}^+, p_{fc}^+),$$
 (9)

$$\Delta = \bar{\Delta} h(p_{ur}^+, p_{dr}^-) , \qquad (10)$$

with f = u, d and c = r, g, b. The functions h(p, q) have been introduced in order to have a common notation for both Model II. One has

$$h(s,t) = \begin{cases} r(s^2) \ r(t^2) & \text{(Model I)} \\ g\left(\left[\frac{s+t}{2}\right]^2\right) & \text{(Model II)} \end{cases}$$
(11)

We have taken into account that, as we will see below, the usual 2SC ansatz implies  $\mu_{fr} = \mu_{fg}$ . In Eq. (7), entries with subindices ur and dr are intended to be multiplied by an  $\mathbf{1}_{2\times 2}$  matrix in rg space, while  $\tau_2^c$  stands for a  $\tau_2$  Pauli matrix acting in this space.

The determinant of  $S^{-1}$  can be analytically evaluated, leading to

$$\Omega^{MFA} = \frac{\bar{\sigma}^2}{2G} + \frac{\bar{\Delta}^2}{2H} - T \sum_{n=-\infty}^{\infty} \int \frac{d^3 \vec{p}}{(2\pi)^3} \sum_{c=r,a,b} \ln \frac{|A_c|^2}{T^8} , \qquad (12)$$

where

$$A_c = (p_{uc}^{+2} + \Sigma_{uc}^2) \left( p_{dc}^{-2} + \Sigma_{dc}^{*2} \right) + (1 - \delta_{bc}) \Delta^2 \left[ \Delta^2 + 2 \left( p_{uc}^{+} \cdot p_{dc}^{-} \right) + 2 \Sigma_{uc} \Sigma_{dc}^{*} \right]. \tag{13}$$

For finite values of the current quark mass,  $\Omega^{MFA}$  turns out to be divergent. The regularization procedure used here amounts to define

$$\Omega_{\text{(reg)}}^{MFA} = \Omega^{MFA} - \Omega^{\text{free}} + \Omega_{\text{(reg)}}^{\text{free}},$$
(14)

where  $\Omega^{\text{free}}$  is obtained from Eq. (12) by setting  $\bar{\Delta} = \bar{\sigma} = 0$ , and  $\Omega^{\text{free}}_{(\text{reg})}$  is the regularized expression for the thermodynamical potential of a free fermion gas,

$$\Omega_{\text{(reg)}}^{\text{free}} = -2 T \int \frac{d^3 \vec{p}}{(2\pi)^3} \sum_{f,c} \left\{ \ln \left[ 1 + e^{-\left(\sqrt{\vec{p}^2 + m^2} - \mu_{fc}\right)/T} \right] + \ln \left[ 1 + e^{-\left(\sqrt{\vec{p}^2 + m^2} + \mu_{fc}\right)/T} \right] \right\} .$$
(15)

The mean field values  $\bar{\sigma}$  and  $\bar{\Delta}$  are obtained from the coupled gap equations

$$\frac{d\Omega_{\text{(reg)}}^{MFA}}{d\bar{\Delta}} = \bar{\Delta} (1 - 16 \ H \ T \ D_{ud}) = 0 , \qquad (16)$$

$$\frac{d\Omega_{\text{(reg)}}^{MFA}}{d\bar{\sigma}} = \bar{\sigma} - 4 G T \left( S_{ud} + S_{du} \right) = 0 , \qquad (17)$$

where we have defined

$$D_{ij} = D_{ji} = \text{Re} \sum_{n=-\infty}^{\infty} \int \frac{d^3 \vec{p}}{(2\pi)^3} h^2(p_{ur}^+, p_{dr}^-) \frac{\Delta^2 + (p_{ir}^+ \cdot p_{jr}^-) + \Sigma_{ir} \Sigma_{jr}^*}{A_r},$$
 (18)

$$S_{ij} = \operatorname{Re} \sum_{n=-\infty}^{\infty} \int \frac{d^{3}\vec{p}}{(2\pi)^{3}} \left\{ 2h(p_{ir}^{+}, p_{ir}^{+}) \frac{\sum_{ir} (p_{jr}^{-2} + \sum_{jr}^{*2}) + \Delta^{2} \sum_{jr}^{*}}{A_{r}} + h(p_{ib}^{+}, p_{ib}^{+}) \frac{\sum_{ib}}{p_{ib}^{+2} + \sum_{ib}^{2}} \right\} .$$
 (19)

So far we have introduced different chemical potentials for each quark flavor and color. However, when the system is in chemical equilibrium not all of them are independent. Within the previously introduced 2SC ansatz, only one color-dependent chemical potential is needed to ensure color charge neutrality. In this way, the  $\mu_{fc}$  can be written in terms of only three independent quantities: the baryonic chemical potential  $\mu_B$ , the quark electric chemical potential  $\mu_{Qq}$  and the color chemical potential  $\mu_B$ . Defining  $\mu \equiv \mu_B/3$ , the corresponding relations read

$$\mu_{ur} = \mu_{ug} = \mu + \frac{2}{3}\mu_{Q_q} + \frac{1}{3}\mu_8$$

$$\mu_{dr} = \mu_{dg} = \mu - \frac{1}{3}\mu_{Q_q} + \frac{1}{3}\mu_8$$

$$\mu_{ub} = \mu + \frac{2}{3}\mu_{Q_q} - \frac{2}{3}\mu_8$$

$$\mu_{db} = \mu - \frac{1}{3}\mu_{Q_q} - \frac{2}{3}\mu_8$$
(20)

Now, in the core of neutron stars, in addition to quark matter we have electrons. Thus, within the mean field approximation for the quark matter, and considering the electrons as a free Dirac gas, the full grand canonical potential is given by

$$\Omega^{full} = \Omega_{\text{(reg)}}^{MFA} + \Omega^e , \qquad (21)$$

where

$$\Omega^e = -\frac{1}{12\pi^2} \left( \mu_e^4 + 2\pi^2 T^2 \mu_e^2 + \frac{7\pi^4}{15} T^4 \right) , \qquad (22)$$

 $\mu_e$  being the electron chemical potential. For simplicity we have neglected here the electron mass.

In addition, it is necessary to take into account that quark matter has to be in beta equilibrium with electrons through the beta decay reaction

$$d \to u + e + \bar{\nu}_e$$
 (23)

Thus, assuming that antineutrinos escape from the stellar core, we must have

$$\mu_{dc} - \mu_{uc} = -\mu_{Q_q} = \mu_e \ . \tag{24}$$

If we now require the system to be electric and color charge neutral, the number of independent chemical potentials reduces further. Namely,  $\mu_e$  and  $\mu_8$  are fixed by the conditions that electric and color densities vanish:

$$\rho_{Q_{tot}} = \rho_{Q_q} - \rho_e = \sum_{c=r,g,b} \left( \frac{2}{3} \rho_{uc} - \frac{1}{3} \rho_{dc} \right) - \rho_e = 0 \quad , \qquad \rho_8 = \frac{1}{\sqrt{3}} \sum_{f=u,d} \left( \rho_{fr} + \rho_{fg} - 2\rho_{fb} \right) = 0 \quad , \tag{25}$$

where

$$\rho_e = -\frac{\partial \Omega}{\partial \mu_e} = -\frac{\partial \Omega^e}{\partial \mu_e} \quad , \qquad \rho_{fc} = -\frac{\partial \Omega}{\partial \mu_{fc}} = -\frac{\partial \Omega_{(\text{reg})}^{MFA}}{\partial \mu_{fc}} \quad . \tag{26}$$

Consequently, in the physical situation we are interested in, for each value of T and  $\mu$  we should find the values of  $\bar{\Delta}$ ,  $\bar{\sigma}$ ,  $\mu_e$  and  $\mu_8$  that solve Eqs. (16) and (17), supplemented by Eqs. (20) and (25).

The electron density can be evaluated analytically, leading to

$$\rho_e = \frac{\mu_e}{3\pi^2} \left( \mu_e^2 + \pi^2 \ T^2 \right) \ . \tag{27}$$

On the other hand, from Eqs. (14), (12) and (15) the quark densities can be expressed as

$$\rho_{(\text{reg})fc}^{MFA} = \rho_{fc}^{MFA} - \rho_{fc}^{\text{free}} + \rho_{(\text{reg})fc}^{\text{free}} . \tag{28}$$

Then a straightforward calculation leads to

$$\rho_{fc}^{MFA} = 2 T \sum_{n=-\infty}^{\infty} \int \frac{d^3 \vec{p}}{(2\pi)^3} \operatorname{Re} \left( \frac{1}{A_c} \frac{\partial A_c}{\partial \mu_{fc}} \right) , \qquad (29)$$

with

$$\frac{\partial A_c}{\partial \mu_{uc}} = -2 \left( i \,\omega_n + \mu_{uc} \right) \left( p_{dc}^{-2} + \Sigma_{dc}^{*2} \right) \left( 1 + 2 \,\Sigma_{uc} \Sigma_{uc}' \right) 
- 2 \left( 1 - \delta_{bc} \right) \Delta^2 \left[ 2 \,\Sigma_{dc}^* \,\Sigma_{uc}' \left( i \,\omega_n + \mu_{uc} \right) + i \,\omega_n - \mu_{dc} \right] 
- 4i \left( 1 - \delta_{bc} \right) \bar{\Delta} \Delta \left[ \Delta^2 + \left( p_{uc}^+ \cdot p_{dc}^- \right) + \Sigma_{uc} \,\Sigma_{dc}^* \right] \frac{\partial h(t, p_{dc}^-)}{\partial t_4} \Big|_{t=p_{uc}^+},$$
(30)

where we have defined  $\Sigma_{fc}'=\bar{\sigma}\left.\partial h(t,t)/\partial t^2\right|_{t^2=p_{fc}^{+\;2}}$ 

The corresponding expressions for  $\rho_{dc}$  are obtained by simply exchanging u and d and taking the complex conjugate, while the expressions for  $\rho_{fc}^{\text{free}}$  can be easily obtained from  $\rho_{fc}^{\text{MFA}}$  by setting  $\bar{\sigma} = \bar{\Delta} = 0$ . Finally,  $\rho_{(\text{reg})fc}^{\text{free}}$  is given by

$$\rho_{(\text{reg})fc}^{\text{free}} = 2 \int \frac{d^3\vec{p}}{(2\pi)^3} \left\{ \left[ 1 + \exp\left(\frac{\sqrt{\vec{p}^2 + m^2} - \mu_{fc}}{T}\right) \right]^{-1} - \left[ 1 + \exp\left(\frac{\sqrt{\vec{p}^2 + m^2} + \mu_{fc}}{T}\right) \right]^{-1} \right\}. \tag{31}$$

### III. NUMERICAL RESULTS

In this section we present our numerical results, showing the features of the phase diagram and the behavior of relevant physical quantities for Models I and II. According to previous analyses carried out within nonlocal scenarios [35], the results are not expected to show a strong qualitative dependence on the shape of the regulator. Thus we will concentrate here on simple and well-behaved Gaussian regulator functions, taking (in momentum space)

$$r(p^2) = \exp(-p^2/2\Lambda^2)$$
 (Model I)

$$g(p^2) = \exp(-p^2/\Lambda^2)$$
 (Model II)

Here  $\Lambda$  is a free model parameter, playing the rôle of an ultraviolet cut-off. We have chosen a different normalization for Models I and II in view of the relation between the respective regulating functions [see Eq. (11)], which determine the low T and  $\mu$  phenomenology.

# A. Parameterization

For definiteness, for both Models I and II we choose here input parameters  $m, \Lambda$  and G which allow to reproduce the empirical values for the pion mass  $m_{\pi} = 139 \,\mathrm{MeV}$  and decay constant  $f_{\pi} = 92.4 \,\mathrm{MeV}$ , and lead to a phenomenologically acceptable value for the chiral condensates at vanishing T and  $\mu_{fc}$ . For Gaussian regulators, taking into account the chosen normalization of the cut-offs, it is seen that within the MFA both models lead to the same expressions for the considered physical quantities at  $T = \mu = 0$ . However, this is not the case when one goes beyond the MFA [39]. In particular, the expressions for the pion mass and decay constant are different (they are still coincident only in the chiral limit), and it is necessary to use different sets of input parameters. The parameters considered here for Model I are m=5.14 MeV,  $\Lambda=971$  MeV and  $G\Lambda^2=15.41$ , while for Model II we have taken m=5.12 MeV,  $\Lambda = 827 \text{ MeV}$  and  $G\Lambda^2 = 18.78$ . With these sets we get for both models a phenomenologically reasonable value for the chiral condensate, namely  $\langle 0|\bar{q}q|0\rangle^{1/3}=-250$  MeV. The remaining free parameter is the coupling strength H in the scalar diquark channel. In order to fix its value by hadron phenomenology at zero T and  $\mu$ , one would have to solve the Faddeev-type equations for baryons as three-quark bound states which result from the quantization of chiral quark models of the type considered in the present paper after bosonization in meson and diquark channels (see [40] and Refs. therein; for more elaborate recent calculations of nucleon properties see [30, 41]). Although in principle this is possible, we refrain from fixing H by hadron phenomenology within the present exploratory study of the quark matter phase diagram and rather choose different values for the coupling ratio H/G, namely  $\frac{1}{2}$ ,  $\frac{3}{4}$  and 1.

# B. Order parameters and phase transitions

For fixed values of the temperature T and the chemical potential  $\mu$  ( $\mu = \mu_B/3$ ), the mean field values  $\bar{\sigma}$  and  $\bar{\Delta}$ , as well as the chemical potentials  $\mu_e$  and  $\mu_8$ , can be numerically obtained from the gap equations (16) and (17), together with the conditions of beta equilibrium and vanishing color and electric charge densities, Eqs. (24-25). Let us begin by considering the case H/G = 0.75, which is motivated by various effective models of quark-quark interactions. Our results for  $\bar{\sigma}$ ,  $\Delta$ ,  $\mu_e$  and  $\mu_8$  are shown in Fig. 1, where we plot these quantities as functions of  $\mu$  for different representative values of the temperature. Left and right panels correspond to Models I and II, respectively. For T=0 (solid lines), at low chemical potentials the system is in both cases in a chiral symmetry broken phase (CSB), where quarks acquire large dynamical masses. By increasing the chemical potential one reaches a first order phase transition in which the chiral symmetry is approximately restored, and the system gets into a phase which is not homogeneous but favors the coexistence of a 2SC phase and a normal quark matter (NQM) phase. In this mixed phase zone the electric neutrality is realized globally: the different phases have opposite electric charges which cancel each other, with a common equilibrium pressure. The chemical potential  $\mu_e$ , which for T=0 vanishes in the CSB phase but is nonzero in the mixed phase, also shows a discontinuity across the transition. As expected, the growth of the color chemical potential  $\mu_8$  in the 2SC component of the mixed phase is approximately proportional to that of the corresponding  $\bar{\Delta}$ , which governs the amount of breakdown of the color symmetry due to quark pairing. When the temperature is increased (see dashed curves in Fig. 1, corresponding to T = 40 MeV), this mixed phase is no longer favored and the system goes into a pure 2SC phase. For T=40 MeV, this shows up as a second order transition in the case of Model I, and a first order transition in the case of Model II. Now, for both models, when one moves along the first order transition line from T=0 towards higher temperatures, one arrives at a triple point (3P). At this point the CSB and 2SC phases coexist with a third, normal quark matter (NQM) phase, in which the chiral symmetry is approximately restored and there is no color superconductivity. Finally, if T is still increased, one reaches an "end point" (EP) where the first order transition from CSB to NQM phases becomes a smooth crossover. The behavior of the dynamical masses and the electric chemical potential  $\mu_e$  along this smooth transition is shown in Fig. 1, see curves corresponding to T = 40 MeV (Model I) and T = 100 MeV (dotted lines, Models I and II).

# C. Quark matter phase diagrams

The described features of the phase diagrams for Models I and II can be visualized in the graphs shown in Fig. 2, where we plot the transition curves on  $T - \mu$  diagrams for different ratios H/G, and show the regions corresponding to the different phases and the position of triple and end points. In the graphs, solid and dotted lines correspond to the mentioned first order and crossover transitions, respectively (in the case of the crossover, the transition point can be defined by considering the maximum of the chiral susceptibility [34]). Between NQM and 2SC regions we find that in all cases there is a second order phase transition, which corresponds to the dashed lines in the diagrams of Fig. 2. Close to this phase border, the dashed-dotted lines in the graphs delimit a narrow band that corresponds to the so-called gapless 2SC (g2SC) phase. Here, in addition to the two gapless modes corresponding to the unpaired blue

quarks, the presence of flavor asymmetric chemical potentials  $\mu_{dc} - \mu_{uc} \neq 0$  gives rise to another two gapless fermionic quasiparticles [11]. Although the corresponding relations cannot be derived analytically owing to the nonlocality of the interactions, the border of the g2SC region can be numerically found. This is done by determining whether for some value of  $|\vec{p}|$  the imaginary part of some of the poles of the Euclidean quark propagator vanish in the complex  $p_4$  plane. In any case, for the range of parameters considered here, this region is found to be too narrow to lead to any sizeable effect.

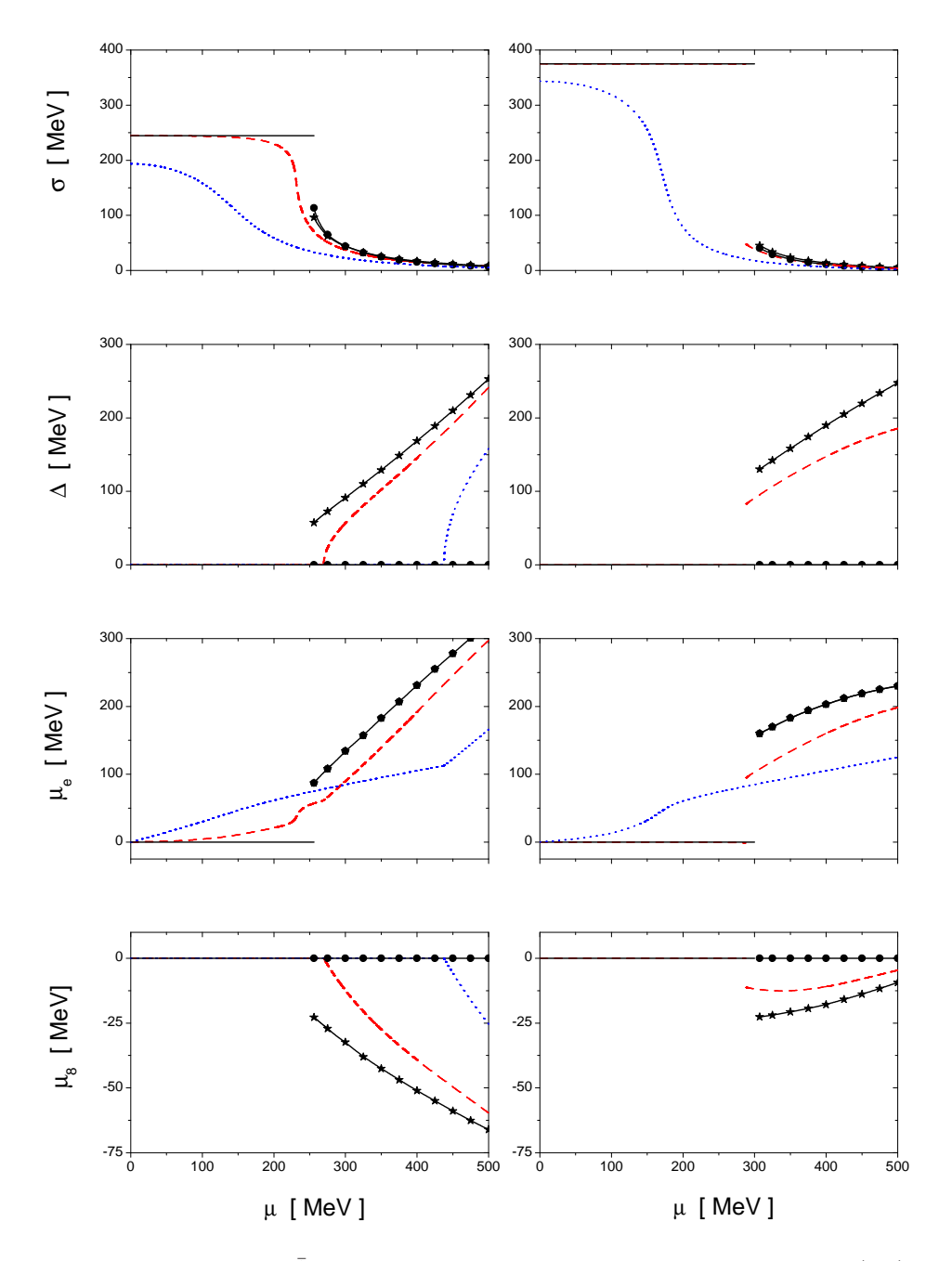


FIG. 1: Behavior of the mean fields  $\bar{\sigma}$  and  $\bar{\Delta}$  and the chemical potentials  $\mu_e$  and  $\mu_8$  for Models I (left) and II (right) as a function of the chemical potential, for three different values of the temperature. The curves correspond to the case H/G=3/4. Full lines correspond to T=0, dashed lines to T=40 MeV and dotted lines to T=100 MeV. In the case of T=0, lines marked with stars and dots correspond to the 2SC and NQM phases respectively.

### IV. DISCUSSION

Let us discuss some qualitative features of the curves displayed in Figs. 1 and 2. On one hand, for both models the 2SC phase region becomes larger when the ratio H/G is increased. This is not surprising, since H is the effective coupling governing the quark-quark interaction giving rise to the pairing. In any case, as a general conclusion it can be stated that, provided the ratio H/G is not too low, these nonlocal schemes favor the existence of color superconducting phases at low temperatures and moderate chemical potentials. Indeed, for the parameters considered here, there is no 2SC phase only in the case of Model II with H/G = 0.5; for Model I, even taking this small ratio some 2SC and g2SC regions can be found at large values of the chemical potential. This is in contrast with the situation in e.g. the NJL model [9, 10], where the existence of a superconducting phase turns out to be rather dependent on the input parameters. In addition, our results are qualitatively different from those obtained in the case of the noncovariant nonlocal models [14], where above the chiral phase transition the NQM phase is preferable for values of the coupling ratio  $H/G \lesssim 0.75$ . In those models, a color superconducting quark matter phase can be found only for  $H/G \approx 1$ .

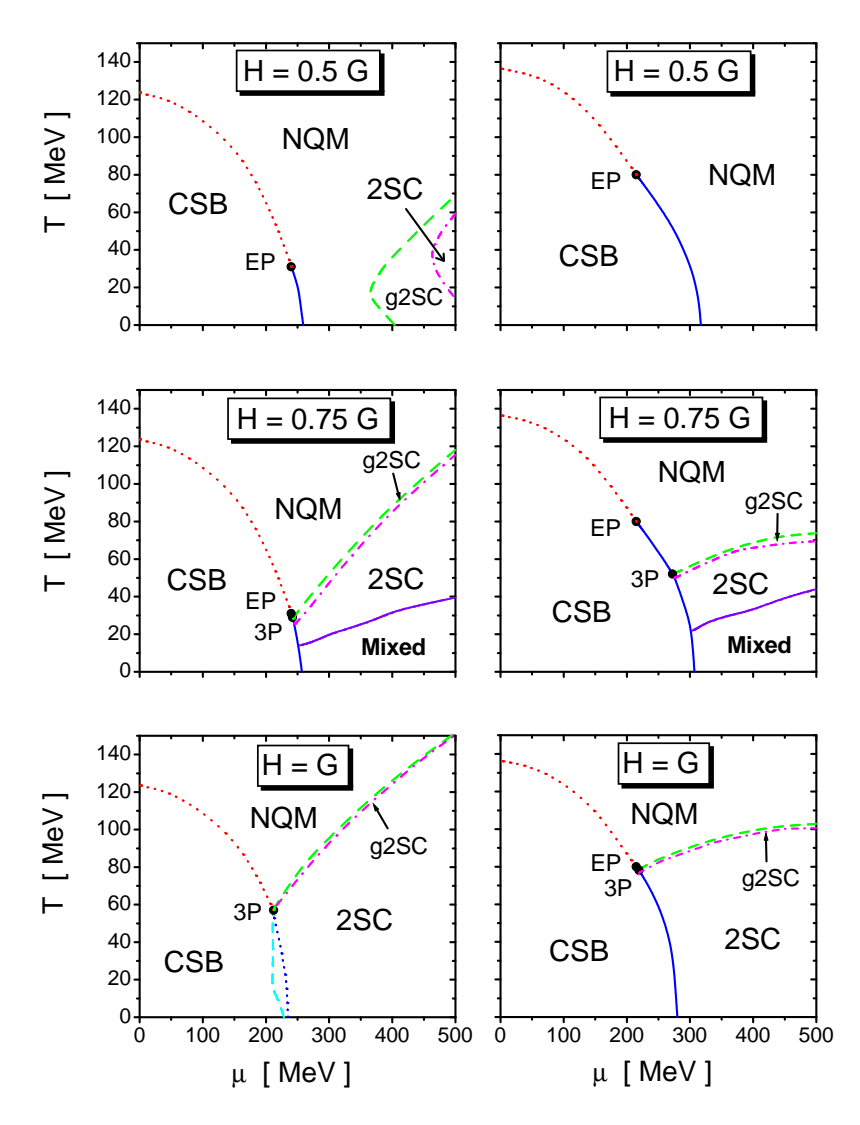
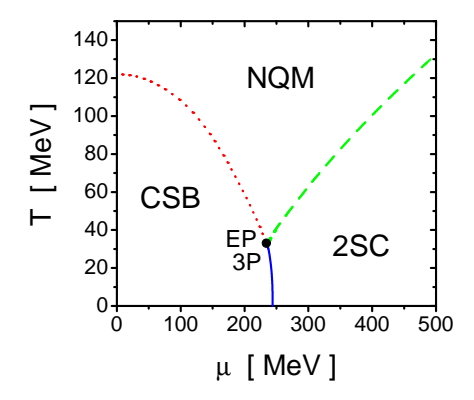


FIG. 2: Phase diagrams for Models I (left) and II (right) for different values of H/G. Full and dashed lines indicate first and second order phase transition curves respectively, dotted lines correspond to crossover-like transitions, and dashed lines delimit the gapless 2SC band. Different phases are denoted as NQM (normal quark matter phase), CSB (chiral symmetry broken phase) and 2SC (two-flavor superconducting phase), while the regions marked as "Mixed" correspond to the NQM-2SC mixed phase. Note that in Model I, for H/G = 1 there is a narrow region in which one has 2SC while the system is still in a chiral symmetry broken phase. EP and 3P denote the end points and triple points respectively.

It is also interesting to compare our results with those obtained for isospin symmetric quark matter. For the same parameter sets, the corresponding phase diagrams for H/G=0.75 are shown in Fig. 3. By comparing them with those of Fig. 2, it can be seen that the 2SC region becomes reduced when one imposes color and electric charge neutrality conditions. This is indeed what one would expect, since the condition of electric charge neutrality leads in general to unequal u and d quark densities, disfavoring the u-d pairing. We notice, however, that the effect is relatively small, and the positions of triple and end points as well as the shape of the critical lines remain approximately unchanged. Concerning the shape of the chiral phase transition line  $T_{\rm CSB}(\mu)$ , one observes at intermediate temperatures  $50~{\rm MeV} \lesssim T_{\rm CSB} \lesssim 100~{\rm MeV}$ , which are relevant for the future CBM experiment, an approximately linear behavior. This can be seen as an interpolation between a convex shape obtained in NJL or bag models and a concave shape for confining Dyson-Schwinger equation models, see e.g. Ref. [42]. It is remarkable that thus in the nonlocal covariant models presented here a similarity with confining quark models occurs and that the chiral/deconfinement transition line in the phase diagram resembles very closely the positions of freeze-out parameters in heavy ion collisions.



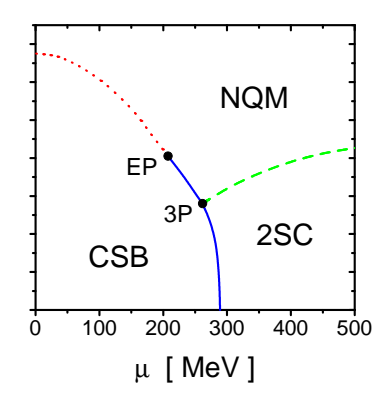


FIG. 3: Phase diagrams for symmetric matter corresponding to Models I (left) and II (right). Here we use H/G = 0.75

Finally, we have studied the dependence of the phase transitions on the model parameters, changing the input value of the chiral condensate within a phenomenologically reasonable range 220 MeV  $\leq -\langle 0|\bar{q}q|0\rangle^{1/3} \leq 280$  MeV. From this analysis, it is seen that the qualitative features of the phase diagrams are not significantly modified. In particular, it is seen that one always finds color superconducting phases at low temperatures and moderate chemical potentials, for intermediate values of the ratio H/G. In addition, the values for the critical temperature at  $\mu=0$  are quite stable, yielding about 120 MeV for Model I and 140 MeV for Model II. This would favor the description given by Model II, in which the result is closer to the values provided by lattice calculations.

### V. CONCLUSIONS

We have considered the phase diagram of two-flavor quark matter under neutron star constraints for two nonlocal, covariant quark models within the mean field approximation. In the first one the nonlocality was due to the regularization procedure, motivated by the instanton liquid model (Model I), whereas in the second model a separable approximation of the one-gluon exchange interaction (Model II) was applied. Although for the Gaussian regulators considered in this work the vacuum gap equations are identical, both models differ in their fluctuation spectrum and therefore in their parameters (current quark mass m, coupling strength G, UV cutoff  $\Lambda$ ) which were fixed by the pion mass, pion decay constant and the chiral condensate. As result of the numerical evaluation of the corresponding gap equations at finite temperature and chemical potential, we have obtained that Model II predicts a larger quark mass gap and a chiral symmetry breaking (CSB) phase transition line which extends 15-20 % further into the  $T-\mu$ plane when compared to Model I. The prediction for the critical temperature at  $\mu = 0$  in Model II,  $T_{\rm CSB} \sim 140$  MeV, is closer to the results of recent lattice QCD simulations than the prediction of both Model I and the well-known local NJL model. We have shown that under neutron star constraints for three values of the coupling strength in the scalar diquark channel (H = 0.5 G, 0.75 G and 1.0 G) different low-temperature quark matter phases can occur at intermediate densities: normal quark matter (NQM), superconducting (2SC) quark matter with a 2SC-NQM mixed phase and pure 2SC quark matter, respectively. The critical temperature for the 2SC phase transition is a rising function of  $\mu$  for the Model I whereas it is rather  $\mu$  independent in the Model II due to the different  $\mu$  dependences associated with the scalar diquark gaps. A narrow gapless 2SC phase appears for medium and large values of the H/G ratio, but in most cases this occurs at nonzero temperatures and thus would not represent a robust feature for compact star applications.

# Acknowledgments

The authors are glad to thank D. Aguilera for useful comments and discussions. This work has been supported in part by CONICET and ANPCyT (Argentina), under grants PIP 02368, PICT00-03-08580 and PICT02-03-10718, and by a scientist exchange program between Germany and Argentina funded jointly by DAAD under grant No. DE/04/27956 and ANTORCHAS under grant No. 4248-6.

- [1] Proceedings of the 17th International Conference on Ultra Relativistic Nucleus-Nucleus Collisions (Quark Matter 2004), Oakland, California, 11-17 Jan 2004, J. Phys. G30, S633 (2004)
- [2] F. Karsch, K. Redlich and A. Tawfik, Eur. Phys. J. C29, 549 (2003)
- [3] E. Shuryak, J. Phys. **G30** S1221 (2004); Prog. Part. Nucl. Phys. **53**, 273 (2004)
- [4] D. B. Blaschke and K. A. Bugaev, Fizika B13 (2004) 491; Prog. Part. Nucl. Phys. 53, 197 (2004)
- [5] K. Rajagopal and F. Wilczek, in At the Frontier of Particle Physics. Handbook of QCD, M. Shifman, ed. World Scientific, Singapore, 2001; M. Alford, Annu. Rev. Nucl. Part. Sci. 51, 131 (2001); D. Rischke, Prog. Part. Nucl. Phys. 52, 197 (2004)
- [6] D. Blaschke, N. K. . Glendenning and A. Sedrakian (Eds.), "Physics of neutron star interiors", Springer, Lecture Notes in Physics 578 (2001); D. Blaschke, D. N. Voskresensky and H. Grigorian, arXiv:hep-ph/0510368.
- [7] M. Alford, K. Rajagopal and F. Wilczek, Phys. Lett. B422, 247 (1998); R. Rapp, T. Schäfer, E.V. Shuryak and M. Velkovsky, Phys. Rev. Lett. 81, 53 (1998)
- [8] M. Alford and K. Rajagopal, JHEP **0206**, 031 (2002)
- [9] M. Buballa, Phys. Rept. **407**, 205 (2005)
- [10] S. B. Rüster, V. Werth, M. Buballa, I. A. Shovkovy and D. H. Rischke, Phys. Rev. D72, 034004 (2005); D. Blaschke, S. Fredriksson, H. Grigorian, A. M. Öztas and F. Sandin, Phys. Rev. D72, 065020 (2005)
- [11] I. Shovkovy and M. Huang, Phys. Lett. **B564**, 205 (2003)
- [12] D. Blaschke, S. Fredriksson, H. Grigorian and A. M. Öztas, Nucl. Phys. A736, 203 (2004)
- [13] H. Grigorian, D. Blaschke and D. N. Aguilera, Phys. Rev. C69, 065802 (2004)
- [14] D. N. Aguilera, D. Blaschke and H. Grigorian, Nucl. Phys. A757, 527 (2005)
- [15] P.F. Bedaque, Nucl. Phys. A697, 569 (2002)
- [16] I. Shovkovy, M. Hanauske and M. Huang, Phys. Rev. D 67, 103004 (2003)
- [17] F. Neumann, M. Buballa and M. Oertel, Nucl. Phys. A714, 481 (2003)
- [18] T. Schafer and E.V. Schuryak, Rev. Mod. Phys. 70, 323 (1998)
- [19] C. D. Roberts and A. G. Williams, Prog. Part. Nucl. Phys. 33, 477 (1994); C. D. Roberts and S. M. Schmidt, Prog. Part. Nucl. Phys. 45, S1 (2000)
- [20] J. Skullerud, D. B. Leinweber and A. G. Williams, Phys. Rev. D 64, 074508 (2001)
- [21] U. Vogl and W. Weise, Prog. Part. Nucl. Phys. 27, 195 (1991); S. Klevansky, Rev. Mod. Phys. 64, 649 (1992); T. Hatsuda and T. Kunihiro, Phys. Rep. 247, 221 (1994)
- [22] E. Ruiz Arriola and L.L. Salcedo, Phys. Lett. B 450, 225 (1999)
- [23] D. Blaschke, Y. L. Kalinovsky, G. Roepke, S. M. Schmidt and M. K. Volkov, Phys. Rev. C53, 2394 (1996)
- [24] G. Ripka, Nucl. Phys. A **683**, 463 (2001); R.S. Plant and M.C. Birse, Nucl. Phys. A **703**, 717 (2002)
- [25] H. Ito, W. Buck and F. Gross, Phys. Rev. C43, 2483 (1991); Phys. Rev. C45, 1918 (1992)
- [26] M. Buballa and S. Krewald, Phys. Lett. B294, 19 (1992)
- [27] R.D. Bowler and M.C. Birse, Nucl. Phys. A582, 655 (1995); R.S.Plant and M.C. Birse, Nucl. Phys. A628, 607 (1998)
- [28] A. Scarpettini, D. Gomez Dumm and N. N. Scoccola, Phys. Rev. D 69, 114018 (2004)
- [29] W. Broniowski, B. Golli and G. Ripka, Nucl. Phys. A703, 667 (2002)
- [30] A.H. Rezaeian, N.R. Walet and M.C. Birse, Phys. Rev. C70, 065203 (2004)
- [31] A.H. Rezaeian and H.-J. Pirner, nucl-th/0510041.
- [32] D. Blaschke and P. C. Tandy, in: "Understanding Deconfinement in QCD", World Scientific, Singapore (2000), p. 218.
- [33] I. General, D. Gómez Dumm and N.N. Scoccola, Phys. Lett. B506, 267 (2001); D. Gómez Dumm and N.N. Scoccola, Phys.Rev. D65, 074021 (2002)
- [34] D. Gómez Dumm and N.N. Scoccola, Phys. Rev. C72, 014909 (2005)
- [35] R. S. Duhau, A. G. Grunfeld and N. N. Scoccola, Phys. Rev. D70, 074026 (2004).
- [36] D. Blaschke, H. Grigorian, A. Khalatyan and D. N. Voskresensky, Nucl. Phys. Proc. Suppl. 141, 137 (2005)
- [37] G. Ripka, Quarks bound by chiral fields (Oxford University Press, Oxford, 1997)
- [38] S. M. Schmidt, D. Blaschke and Y. L. Kalinovsky, Phys. Rev. C50, 435 (1994)
- [39] D. Gómez Dumm, A.G. Grunfeld and N.N. Scoccola, in preparation.
- [40] R. T. Cahill, Nucl. Phys. **A543**, 63C (1992), and Refs. therein.
- [41] R. Alkofer, A. Holl, M. Kloker, A. Krassnigg and C. D. Roberts, Few Body Syst. 37, 1 (2005)
- [42] D. Blaschke, C. D. Roberts and S. M. Schmidt, Phys. Lett. B 425, 232 (1998)